

Article

An Image Processing-Based Method to Analyze Driver Visual Behavior Using Eye-Tracker Data

Furkan Aydin ¹, Giandomenico Caruso ^{2,*} and Lorenzo Mussone ¹

¹ Department of Architecture, Built Environment and Construction Engineering, Politecnico di Milano, 20133 Milan, Italy; furkan.aydin@mail.polimi.it (F.A.); lorenzo.mussone@polimi.it (L.M.)

² Mechanical Department, Politecnico di Milano, 20156 Milan, Italy

* Correspondence: giandomenico.caruso@polimi.it; Tel.: +39-02-23998094

Abstract: This paper presents a practical method for analyzing drivers' eye movements, providing a valuable tool for understanding their behavior during driving simulations. The method, which utilizes an image processing technique, addresses the challenges when the driver's attention is on points without information about the image depth. The screen image changes or moves with the simulation. It allows us to identify the gaze position relative to the road, determining whether the glance is inside or outside. This is achieved by transforming RGB images (frames) collected by the eye-tracker video camera into a b/w image using the Canny filter. This filter can identify objects' contours by evaluating the change in color of their surfaces. A window is then applied to these new images to extract information about the gaze position in the real world. Four drivers were used as a sample for the method's testing. The findings demonstrate various driver variations and a disparity between driving in curved and rectilinear segments. The gaze is typically inside the road in curved sections, whereas in rectilinear sections, the gaze is frequently outside.

Keywords: gaze analysis; driver behavior; image processing; driving simulator; eye-tracker



Citation: Aydin, F.; Caruso, G.; Mussone, L. An Image Processing-Based Method to Analyze Driver Visual Behavior Using Eye-Tracker Data. *Appl. Sci.* **2024**, *14*, 6123. <https://doi.org/10.3390/app14146123>

Academic Editors: Roland Jachimowski, Michał Kłodawski and Suchao Xie

Received: 20 April 2024

Revised: 27 June 2024

Accepted: 11 July 2024

Published: 14 July 2024



Copyright: © 2024 by the authors. Licensee MDPI, Basel, Switzerland. This article is an open access article distributed under the terms and conditions of the Creative Commons Attribution (CC BY) license (<https://creativecommons.org/licenses/by/4.0/>).

1. Introduction

One of the most important contributing factors to traffic crashes is driver behavior, which has been the subject of numerous investigations. This activity may now be accomplished while considering various potential danger conditions in a perfectly safe driving environment, thanks to driving simulators. Examining drivers' eye movements is critical as a sign of their focus and readiness to operate a motor vehicle. The number of vehicles is continuously rising, and road crashes have increased in frequency and severity, becoming one of the world's leading causes of mortality [1]. Despite advances in improving the regulation of important risk factors, road crashes remain a primary cause of death and serious injury in many developed and developing nations. According to the World Health Organization (2018) [2], road traffic crashes cost the lives of over 1.35 million people globally each year. Road traffic injuries are the eighth biggest cause of mortality for people of all ages. Human error is a common cause of traffic crashes, which becomes more likely as a driver's cognitive ability deteriorates [1]. According to the European Commission's road safety manual (European Commission) [3], motor vehicle crashes are caused by a combination of human, vehicle, and environmental factors.

Mental workload (MWL) is one indicator that may be used to evaluate human-machine interaction, and it is an essential design paradigm for investigating human-technology interactions [4]. Pupil diameter change [5], blink duration [6], horizontal gaze dispersion [7], blink frequency [8], gaze duration, saccade number [9], standard deviation (SD) of horizontal eyeball rotation [8], and variations in gaze points [10] have been proposed as powerful indicators of MWL among the numerous eye-tracking measurements.

Moreover, driver distraction is "the diversion of attention away from activities vital to safe driving and toward a competing activity" [11]. It is also becoming recognized as a

contributing cause of many vehicle crashes [12–15]. Eye tracking technology is valuable for measuring mental workload and driver distraction by examining visual attention and gaze behavior. Changes in gaze behavior have been observed to reflect varying cognitive demands, offering insights into the mental demands of a task. Similarly, longer fixation durations and less frequent fixations have been observed in distracted drivers performing secondary tasks. These changes can be used to develop objective measures of driver distraction and to design safer human–machine interfaces [16,17].

According to data analysis from the 100-car naturalistic driving study of adult drivers, the probability of road crashes or near-crashes rose with eye glances away from the forward roadway lasting more than two seconds. The data from this naturalistic investigation were subjected to further analysis. The results showed a correlation between the likelihood of a crash and the total or cumulative duration of eye movements away from the forward roadway [18].

In another study, using advanced gravitational force detection techniques, 42 new teenage drivers had equipment installed in their cars to monitor crashes and near-crash events (CNCs). Video footage from the six seconds before each CNC and randomly selected non-CNC road segments were coded to determine the length of eye glances off the front roadway and the existence of secondary task engagement. A more reliable indicator of a distraction than the single most prolonged glance was the total duration the eyes were off the forward roadway. Generally, the longer the distraction, regardless of activity, the greater the CNC risk [19].

To enhance road safety, it is essential to investigate drivers' behavior and identify their weaknesses. This will help to identify critical situations when drivers are distracted by secondary tasks or gaze-related activities.

This study aims to develop a method for analyzing gaze and determining where drivers look at the road simulation scenario rather than just on the simulation's screen. The exact position on the screen may show different points of the scene according to simulation dynamics. The presented approach is based on an image processing technique that can recognize the boundaries of the road and, to them, the point where the driver is looking, whether inside or outside the road section. Our research is driven by the need to directly integrate eye-tracking data with simulation to analyze driver behavior comprehensively. The analysis of eye-tracker video recordings alone presents limitations due to the lack of correlation with the simulation environment. To overcome this, we propose a method that links eye-tracking data with simulation in virtual reality settings. This approach efficiently analyzes driver gaze data, even with devices lacking depth and lane data, offering advantages in understanding driver behavior and attention allocation. Examining gaze positions at road borders, our study aims to significantly enhance understanding of driver cognition and contribute to substantial improvements in road safety measures.

The paper includes five other sections. In Section 2, a review of papers about the driver's visual behavior and its relationship with driving attention is carried out; in addition, the techniques used to analyze glance data are also presented here. In Section 3, the Methodology adopted for the analysis is described. The results are presented in Section 4 and then discussed in Section 5. Finally, in Section 6, the Conclusions are drawn.

2. Literature Review

Several studies demonstrate that driving context could influence drivers' glance behavior [20,21]. Studies have been conducted to evaluate both the effect of the duration of the occlusion and the different road conditions on the driver's attention [22]. Green (2002) [23] highlighted that driving on curves is riskier than driving on straight roads, and one would anticipate some shift in fixation distributions because of curvature. Driving on curves has garnered much attention, partly because it is more complex than driving on straight segments and partly because collisions are more probable. Drivers spend more time gazing at the edge lines when driving on curves than when driving straight ahead to obtain essential guiding signals. According to Olson et al. (1989) [24], the

time spent on the inner road edge climbs from around 10% for a straight stretch to roughly 30% for left curves and 40% for right curves of unknown radius. Drivers have a higher preview distance for wider curve radii, typically staring toward the vanishing point and scattering their fixations over a larger region [25,26]. Drivers on sharper road curves looked at the forward road more frequently and longer [27].

Another study [28] investigated where drivers glance when approaching bends on a twisty road. Prior models of visual processes in curve driving have concentrated on path-control behavior. The occlusion point of a curve was defined in the study as the nearest point where the vision of the road was covered by some barrier (e.g., due to wild vegetation). The study revealed that drivers approach open bends on rural roads and look towards the occlusion point.

Safe driving depends on appropriate visual behavior. Drivers who engage in non-visual cognitive tasks tend to focus more on the road ahead (on-path glances), neglecting off-path hazards, worsening scanning patterns, and increasing the risk of missing critical information about potential dangers [29]. Vision is crucial for lane keeping and path planning in low-traffic driving scenarios, with the gaze typically fixed on a target point determined by future car position. In complex environments like urban areas, vision is needed to monitor other drivers and traffic signs. Due to human vision's limited accuracy outside the foveal area, drivers must shift their gaze between the projected route and surrounding objects [28]. A shift in the fixation pattern is a more qualitative distinction between straight and curved parts. According to the research by Bengler et al. (1996) [30], a significant percentage of changes left and right are often seen at a fair distance in front of the car when driving in bends.

Though similar patterns are also present in curve fixation patterns, the prevailing pattern for straight portions is thought to entail more of a straight-ahead close-far variety. Zwahlen (1993) [31], for instance, claims that the typical fixation pattern creates a series of fixes, each of which entails gazing incrementally farther down the road before making a fixation closer to the vehicle to resume the sequence. There is a tendency to glance towards the inside of curves, mainly right-hand curves. However, it is essential to note that sight distance is typically shorter along the curves' interior than the exterior. Detection of targets depends on frequent gaze direction, with curves on the right side receiving more attention, especially from experienced drivers at higher speeds. According to the study by Shinar et al. (1977) [32], a curve has more intense visual search activity than a straight line. When drivers are not looking at the road, crash risk is increased. In the paper by Green (2002) [23], the expected number of fatalities from an in-vehicle task can be predicted from a combination of the number of glances at the device per use, the mean glance duration, and the frequency of device use per week.

Hristov (2019) [33] assessed the gaze behavior during actual trips by test subjects utilizing a measurement vehicle equipped with an exact "Smart Eye Pro" remote eye-tracking system using corneal reflection. The researchers plotted the fixation distributions in straight portions and the right and left curves. The study concludes that driver stress is higher in bends than on straight stretches, resulting in increased attention. Specific patterns distinguish the gaze behavior on the left and right horizontal curves. On straight lines, the driver's sight is nearly uniformly spread throughout the whole width of the road. Compared to straight stretches, a reduced gaze dispersion might be achieved when driving through bends. Curves, on the other hand, have a more intense quest for information. The study revealed that horizontal curves cause higher eye stress and concentration than straight segments.

Due to their inexperience and limited field of vision, inexperienced drivers are more likely to misunderstand the information they gather while driving. The results showed that, compared to experienced drivers, novice drivers displayed a higher dwell time on traffic signals, pedestrians, and passing cars, as well as a longer fixation duration on the dashboard and navigation system [34]. Previous studies have revealed that beginner and expert drivers differ in various ways. In general, novice drivers have less developed vehicle control

abilities and fewer spare attentional capacities than expert drivers [35,36]. For instance, crash rates are high in the first few months after obtaining a driver's license and decline as drivers gain experience [37,38]. Furthermore, rookie drivers have a worse capacity to perceive and predict traffic hazards than experienced drivers [39,40]. Additionally, inexperienced drivers tend to fixate on the local area more frequently, depend less on peripheral vision for vehicle control, and adjust their visual search less successfully to the environmental conditions [41–44].

The research by van Leeuwen et al. (2015) [45] examined how 52 inexperienced drivers' driving abilities and gaze patterns changed as they gained experience in the simulator. The participants drove as close as possible to the middle of the right lane over four sessions of six to eight minutes each on a rural road with several 90-degree turns. The eye-tracking data revealed that participants stretched their visual search more and reduced gaze tunneling. Gaze tunneling involves focusing on a single point instead of scanning the surroundings and happens when drivers are stressed or engaged in tasks such as navigating or reading signs. This behavior is dangerous, as it can lead to missed hazards and a higher likelihood of collisions. In the study by Hristov (2019) [33], the researchers used the parameter "scan route length" to measure gaze tunneling by determining the length of the driver's gaze path. Moreover, the results show that from the first to the fourth session, the standard deviation of lateral position (SDLP) and steering activity dramatically reduced, gaze variation rose, and self-reported workload decreased.

Hornig et al. (2004) [46] presented a vision-based real-time driver weariness monitoring system for safe driving. Image processing methods, such as the HSI color model, were employed in this study to detect faces in input photos, and the Sobel edge operator was used to estimate eye positions and produce eye images as dynamic templates for eye tracking. In the study, the system's eye recognition and tracking had an average accuracy rate of 99.1%, correctly detecting all instances of human-marked fatigue. Regarding identifying driver fatigue, the system has an accuracy rate of up to 88.9%.

Ohn-Bar and Trivedi (2014) [47] employed image processing algorithms to establish a vision-based system for categorizing hand motions that uses a combined RGB and depth descriptor. The method was being investigated for use in vehicles for human-machine interaction. A hand detection and user determination step were used first to demonstrate a comprehensive system, followed by a real-time spatiotemporal descriptor and gesture classification technique. A collection of 19 gestures was divided into four subgroups for use in diverse interactive applications. The dataset used in the study presented challenges due to variations in hand motions and lighting conditions. To address these challenges, the researchers tested multiple temporal descriptors and discovered that combining RGB and depth information (RGBD fusion) was an effective method for accurately identifying hand gestures.

Zhang et al. (2017) [48] proposed a computation technique employing the PERCLOS (percentage of eye closure time) parameter based on machine vision to determine whether a driver's eyes were fatigued. The recommended approach for evaluating driver fatigue utilizes image processing and provides rapid calculation, high detection, and precision in recognition. Xi and Zhang (2018) [49] designed a safety feature detection system to ensure the safety of long-distance transportation by detecting fatigued driving, distracted driving, and uncontrolled driving. Eigenface, Fisher Face, and LBPH image processing algorithms provided a 100% face recognition rate. Histogram of Oriented Gradients (HOG) and Support Vector Machine (SVM) algorithms delivered an 80% recognition rate for recognizing drivers' mobile phones.

3. Methodology

This section provides an overview of the survey environment and the procedures adopted in the experiments for using the eye tracker and driving simulator. The collection and preliminary analysis of eye-tracker data were reported. Additionally, the method

for processing the frames of the simulation video was thoroughly discussed, along with definitions of the guidelines for an appropriate gaze analysis.

3.1. The Experimental Setup

A driving simulator was utilized to conduct tests on a driving scenario with manifold aims besides the eye-tracker analysis. The specific eye-tracker testing phase involved four participants, and the data collected during the testing was analyzed using the newly proposed methodology. The driving simulator used in the experiment is made up of a fixed seating buck, a set of vehicle controls (force-feedback steering wheel, gear shifter, and pedals), and three 32" full-HD monitors with a 175-degree field of view to display the virtual driving scenario (Figure 1). The IPG Automotive CarMaker 7.0.3 (CarMaker, 2024) [50] software was used to simulate the scenarios. CarMaker is a vehicle simulation software with intelligent driver models, detailed vehicle models, and highly adaptable road and traffic models.



Figure 1. The driving simulator during the experimental test.

The Politecnico di Milano Campus Bovisa, La-MASA district, located northwest of Milan, is the case study application for evaluating the proposed analysis method. The modeled area is 350 m × 350 m wide, and the driving simulation path is 1.12 km long, corresponding to the public one-way ring road that travels along and between the university area. The area consists primarily of isolated structures (university buildings) surrounded by open spaces and fences.

The 3D models utilized in this study were created using the SketchUp 3D 2019 design software (SketchUp, 2019) (Figure 2).

A digital camera was used to take images of visible facades from the road. An identical route was proposed for all participants. The route was solely designed to be driven in a counterclockwise orientation. The speedometer display was visible in the top left corner of the screen.

The survey involved 4 participants aged between 21 and 26 years with driving experience between 2 and 5 years. All the participants hold valid driver's licenses. The drivers were identified as #1, #2, #3, and #4. The ethical committee of Politecnico di Milano approved the survey protocol.

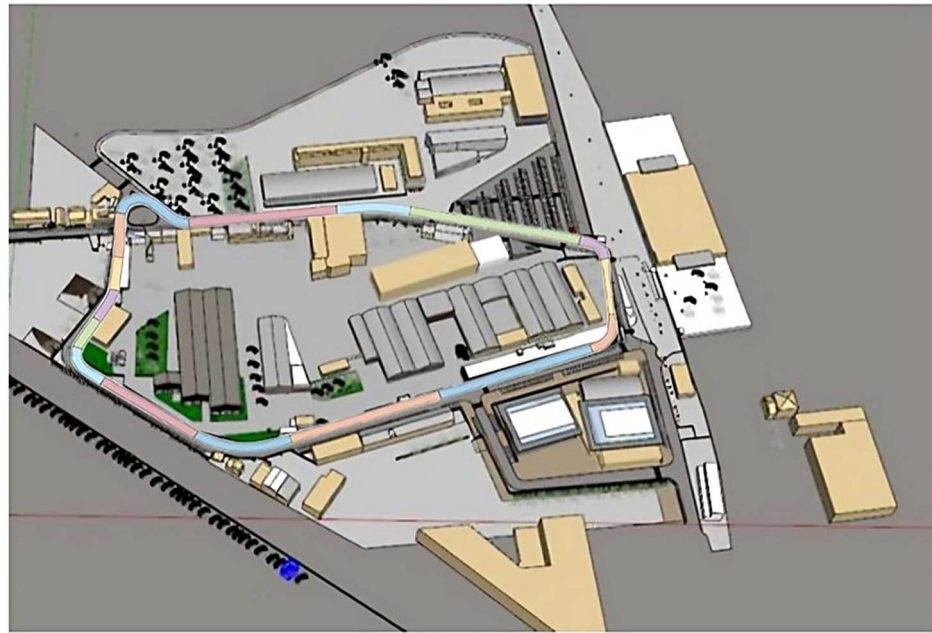


Figure 2. A SketchUp 3D design of the La Masa area, Bovisa Campus.

3.2. The Procedure of the Experiment

Participants were first asked to sign an informed consent form, which outlined the procedures and tasks of the experiment. After some preliminary activities, they completed a questionnaire on their social information, and the eye-tracker glasses were worn. All drivers run through the path of the testing scenario twice. The road section was divided into eight straight and eight curved portions based on the road radius ratio. Figure 3 represents the road segments with numbers ranging from 1 to 16. Segments 2 and 5 (the curvilinear and rectilinear, respectively) were then selected for the following analysis.

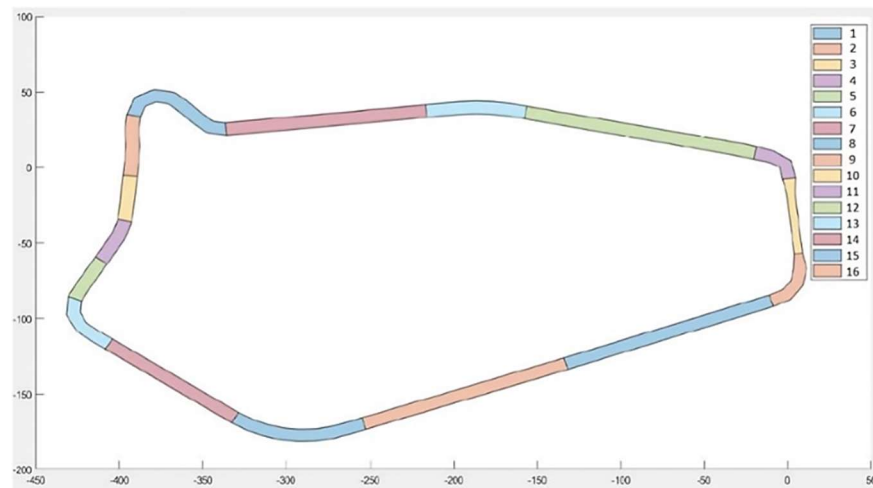


Figure 3. The road circuit's segmentation. The rectilinear segment 5, and the curvilinear segment 2 were selected for the analysis.

3.3. Data Collection and Pre-Processing

The Pupil Labs eye tracker device's handbook describes the World Camera as the physical scene camera that records the subject's field of vision (called world video), referring to the driver's perspective. The world video was acquired from the Pupil Labs 3.0 software, together with the timestamps of each frame. Because the gaze locations are given in 2D normalized space, a program was built to convert them to 2D image space. To determine the

exact position of the gaze on the image of the frames, the gaze coordinates were projected onto the image frame of 1280×720 pixels. Consequently, precise gaze positions on the frame photos were obtained. Constructing a reference array addressed the difference in timestamps between gaze locations and video frames. This reference array facilitated the selection of the nearest frames and gaze positions to a new reference array that still had a 100-millisecond time step. The choice of this time step for the reference array was aligned with the CarMaker vehicular data sampling time step. The matching procedure involved filtering the nearest time steps of the frames and gaze positions based on the reference array. The results of the matching procedure indicated a satisfactory degree of precision, with the most significant error being on the order of 10 milliseconds. An example of the matching procedure is provided in Table 1, where the accuracy ($| \text{gaze_time} - \text{frame_time} |$) column displays the errors, and the frame_time and gaze_time columns display the time steps of the nearest frames and gaze positions chosen relative to the reference array.

Table 1. A partial listing of nearest frame timestamps to gaze position timestamps for segment 2.

Segment	Gaze Location in the X-Axis	Gaze Location in the Y-Axis	Time (Reference)	Gaze_Time	Frame_Time	Accuracy	Frame_Number
2	677.391	415.385	103.2	103.204	103.195	0.0087	4861
2	677.391	415.385	103.3	103.300	103.296	0.0041	4866
2	677.391	415.385	103.4	103.396	103.396	0.0004	4872
2	677.391	415.385	103.5	103.501	103.514	0.0130	4878

This sequence of operations is synthesized in the flow chart in Figure 4. Table 2 reports the total number of available frames and those used for the analysis. It is easy to see that the percentage of frames analyzed in the curvilinear segment is generally lower than in the rectilinear one due to the substantial change in the driver's perspective and the shorter length of the curvilinear segment. Obstructions to the driver's view, such as the front and side windows or side-view mirrors, may prevent the capture of road boundary coordinates, resulting in frames where one or both road borderlines cannot be discerned and are excluded from the analysis. In addition, the analysis utilized only a tiny fraction of the total frames in the segments, ranging from 9% to 22%. This limited proportion was mainly caused by the need to match eye-tracker video camera frames with vehicular data sampled at a 100-millisecond timestep.

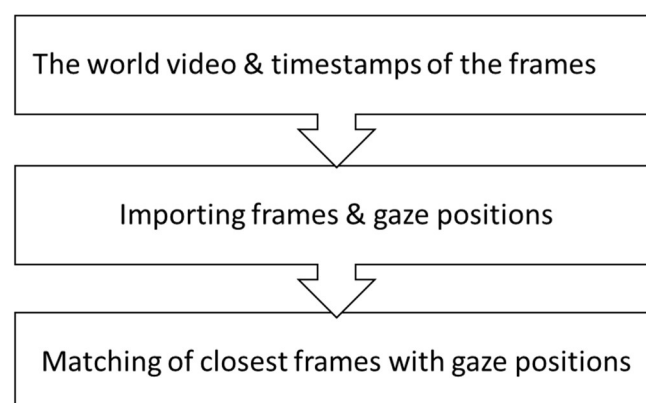


Figure 4. Flowchart summarizing the matching of eye-tracker video camera frames with vehicular data.

Table 2. Statistics of total vs. functional and analyzed eye-tracker video camera frames.

Segments	Driver #1		Driver #2		Driver #3		Driver #4	
	# of Total Frames	# (%) of Analyzed Frames	# of Total Frames	# (%) of Analyzed Frames	# of Total Frames	# (%) of Analyzed Frames	# of Total Frames	# (%) of Analyzed Frames
Segment 5, Rectilinear	443	96 (22%)	734	133 (18%)	650	135 (21%)	579	113 (20%)
Segment 2, Curvilinear	187	30 (16%)	296	27 (9%)	109	24 (22%)	232	22 (9%)

3.4. Image Processing

There are four types of representations to show the pixels of an image: grayscale, binary, color (RGB), and indexed color. A grayscale or binary pixel has one data value, and a color pixel has three data values (each for one of the color channels). Additionally, an indexed color image has one data value per pixel, which is an index for a color map.

The frames collected by the world camera were picked to be evaluated to compare gaze positions and road borders to identify the driver's gaze position and whether it was inside or outside the road limits during the driving session. Figure 5 proposes one frame with the point of the gaze (the red dot in the center of the green circle).

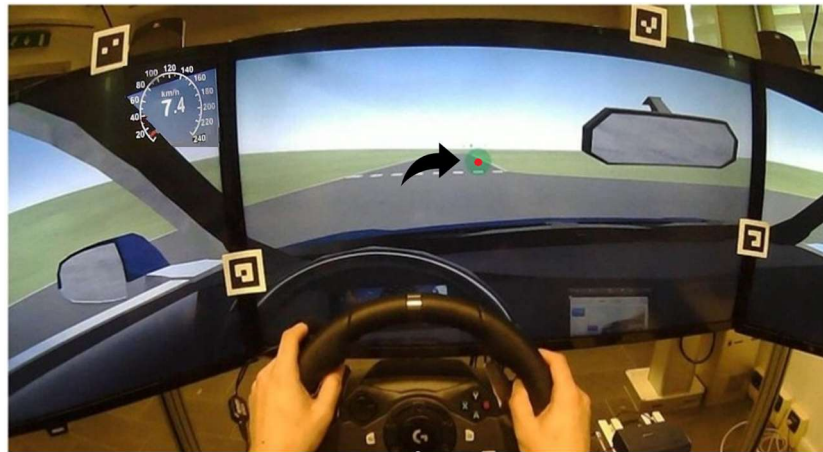


Figure 5. This is an example of the frame image before processing. The red dot inside the green circle (pointed by the black arrow) represents the gaze.

To determine the road borders in the image, first, the RGB image was converted into a grayscale image, and then the Canny algorithm (Canny, 1986) [51] was used to detect the edges in the image, which also included the borders of the road. Figure 6 shows an example of an image frame after it has been converted from an RGB image to a grayscale image. The Canny algorithm was applied to each extracted image, and the locations with a significant color shift in the images were detected. It is a function that searches for local maxima of the gradient of the input image to detect edges. This approach detects solid and weak edges using two thresholds and includes weak edges in the output if they are related to solid edges. The Canny approach is less likely than other methods to be deceived by noise and more likely to detect actual weak edges, thanks to the use of two thresholds. However, this study utilized the Canny edge detection algorithm with a single threshold value to identify and include solid edges in the output binary image. This threshold value was selected based on the maximum edge strength that should result in a grayscale image. Consequently, any edge with a strength greater than the chosen threshold value was considered a solid edge and included in the output image. The driver gaze position was acquired after converting the gaze positions from 2D normalized to 2D image space (Section 3.3).

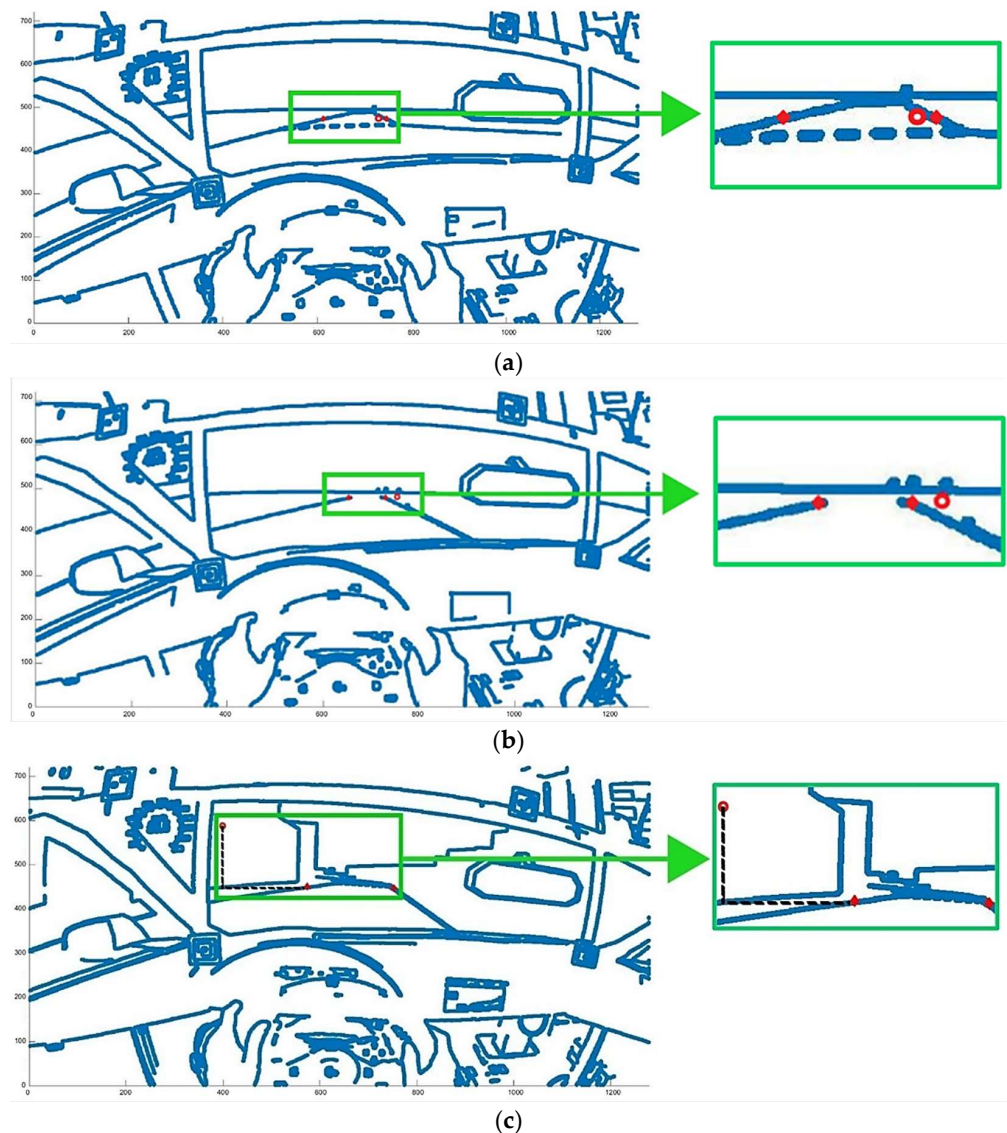


Figure 6. The three cases considered to pinpoint the gaze (the red dots and circles magnified on the right) are as follows: (a) the gaze is inside the road; (b) the gaze is outside the road, and there are no buildings; and (c) the gaze is outside the road on the facade of a building.

Figure 6 illustrates a processed image of a frame from a world movie with all identified edges and the driver's gaze location. The Canny algorithm generates a binary picture filled with 1 and 0 values. The pixels with value 1 in the frame are known as image edges; these are the image portions where color transitions occur.

Here, we explain the algorithm used to pinpoint the gaze.

The primary hypothesis is that the gaze refers to a point on a plane belonging to a relatively wide object; this object can be the road surface, a vertical sign, a building facade, or a generic wall.

The images from the simulation are in 2D, so we need further information to obtain the third dimension. This is achieved by using the buildings whose bases, in our scenario, lie on the same road plane. We use the same binary picture generated by the Canny algorithm to determine the basis of buildings.

We identify three prominent cases shown in Figure 6:

- (a) The gaze is inside the road; the roadside y-coordinates are the same as the gaze;

- (b) The gaze is outside the road, and there are no buildings. The roadside y-coordinates (in the frame space) are the same as the gaze. Some errors may be inserted due to perspective distortions, especially if the gaze is far from the road;
- (c) The gaze is outside the road, on the facade of a building; the projection of the gaze on the base of the building and the roadside y-coordinates are the same. Some errors may be inserted due to the inaccurate definition of building boundaries, especially when shades hide them.

A selection window was created to choose the road borders from the image's edges. Its size must be large enough to include only the roadsides, and the height must be as small as possible to avoid errors in detecting the y-coordinates. However, the driver's perspective is influenced by various factors such as head movement, vehicle position, and orientation, which makes it challenging to maintain a consistent selection window. To overcome this issue, the selection window was designed to adjust to the constant shifts in the driver's perspective. The selection window's size and placement were kept as consistent as possible to evaluate more frames with proper road border coordinates. Despite the efforts to keep the selection window consistent, maintaining the same window in curvilinear segments of the circuit is hindered by the significant shift in the driver's view caused by the road curvature radius. A larger radius of curvature leads to a more significant shift in the driver's viewpoint.

The flow chart in Figure 7 reports the image processing procedure executed on each frame to detect the road borderlines.

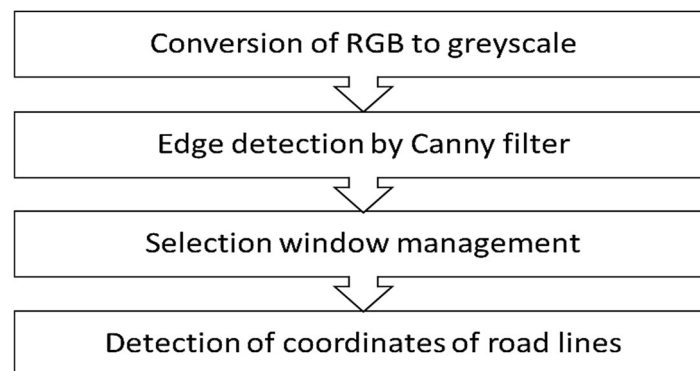


Figure 7. Flowchart of a summary of the image processing procedure for the detection of road borderlines.

Another critical issue that should be addressed for some of the frames, particularly in the curvilinear segments, is that sometimes the roadsides are not included in the driver's view because the vision of one or both of the road boundaries is entirely covered by the frame of the front and left or right windows of the vehicle, and other times by the side-view mirrors of the vehicle. In these situations, capturing the road boundary coordinates is impossible due to visibility limitations. Since there was no way to discern one of the road borderlines or both, these frames were not included in the analysis.

As mentioned, many elements affect the driver's perspective, including head movement, curvature radius, vehicle location and orientation along the circuit path, and so on. Detecting points on the road borderlines is impossible due to either a blockage by the vehicle's window frames or the absence of one of the road borderlines in the image due to the driver's perspective (Figure 8).

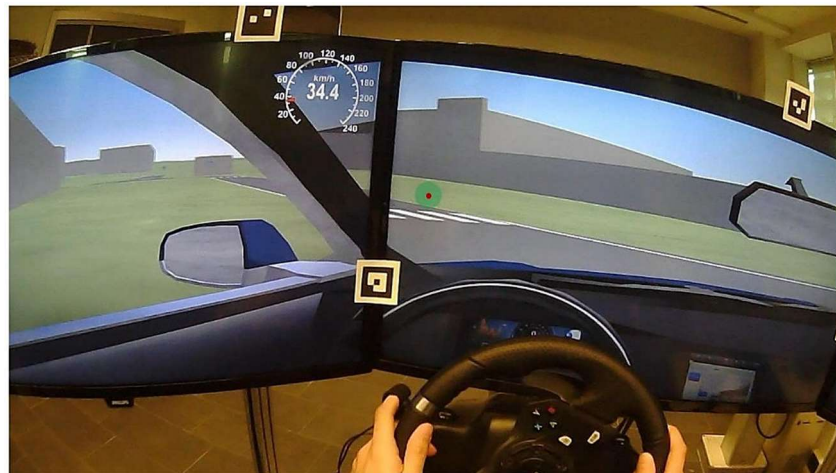


Figure 8. The frame image shows where the vehicle window frame obstructs the visibility of the road's left borderline.

3.5. Gaze Analysis

After the road boundaries were identified, to comprehend whether the driver's gaze is within or outside the road, the following calculations were conducted using the coordinates of the gaze and the roadsides (assuming that the origin of the axes is located on the roadside at right). By computing the distance between the gaze coordinates and the coordinates of the right roadsides, it is possible to identify whether the gaze is within or beyond the road boundaries.

Figure 9 shows the image of the processed frame with the gaze point (red circle), whereas Figure 10 depicts the details of Figure 9 concerning the calculation of variables *a* and *b*. Distance *a* is the horizontal distance between the driver's gaze and the roadside at the right, whereas distance *b* represents the road width in the image (Figure 11). It is worth noting that the actual value of *b* is known. After *a* and *b* were calculated, the variable ratio was calculated as the ratio between *a* and the absolute value of *b*:

$$\text{ratio} = a / \text{abs}(b) \quad (1)$$

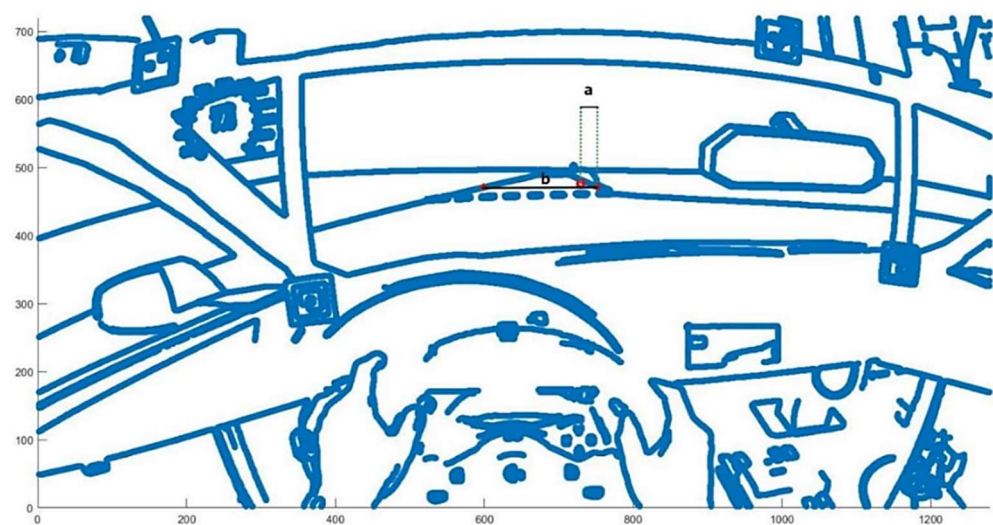


Figure 9. A processed image shows the distances *a* and *b* (see Figure 10 for details).

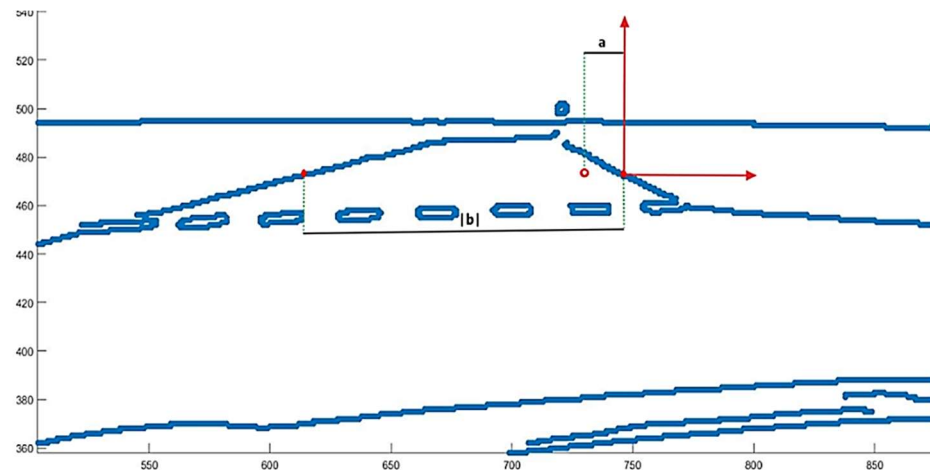


Figure 10. Processed image with the reference origin chosen as the right borderline of the road. The distance a is the horizontal distance between the driver's gaze and the roadside at the right. The distance $|b|$ represents the absolute value of the road width.

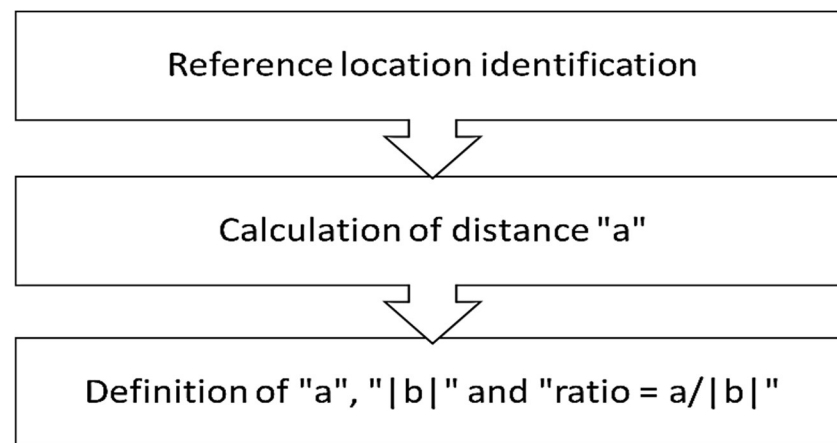


Figure 11. The sequence of operations to obtain a , b , and ratio.

By analyzing the variable ratio, we can draw the following rules:

- If the ratio is < 0 and the ratio is > -1 , the gaze is assumed to be inside the road.
- If the ratio is > 0 or the ratio is < -1 , the gaze is assumed to be outside the road.
- If the ratio = -1 , the gaze is on the left road borderline.
- If the ratio = 0 , the gaze is on the right road borderline.

We can calculate the location of gaze in the real world, a' , because we know the real value b_{real} of b , which in turn is affected by perspective. According to Equation (2), we could compare the gazes along a hypothetical section of the road by using this linear transformation:

$$a' = (a/b) \times b_{\text{real}} \quad (2)$$

Thresholds were defined using a constructed selection window to choose the road limit pixel coordinates on the x -axis. They were updated according to the subsequent considerations necessary to accurately interpret the driver's gaze.

The selection window must always be adjusted with proper thresholds, especially in critical situations, such as when the driver's gaze is very close to the right borderline of the road. This is because the perspective in those cases (driving counterclockwise) can lead to an incorrect interpretation of whether the gaze is inside or outside the road. The following Figure 12 provides an example of such a scenario. If the chosen road boundary pixels have a lower value on the y -axis (closer to the vehicle), the interpretation would be that the gaze is inside the road boundaries, which would be incorrect. Because of this, it is necessary

to precisely arrange the selection window that picks the road margins, especially in those kinds of unique situations.

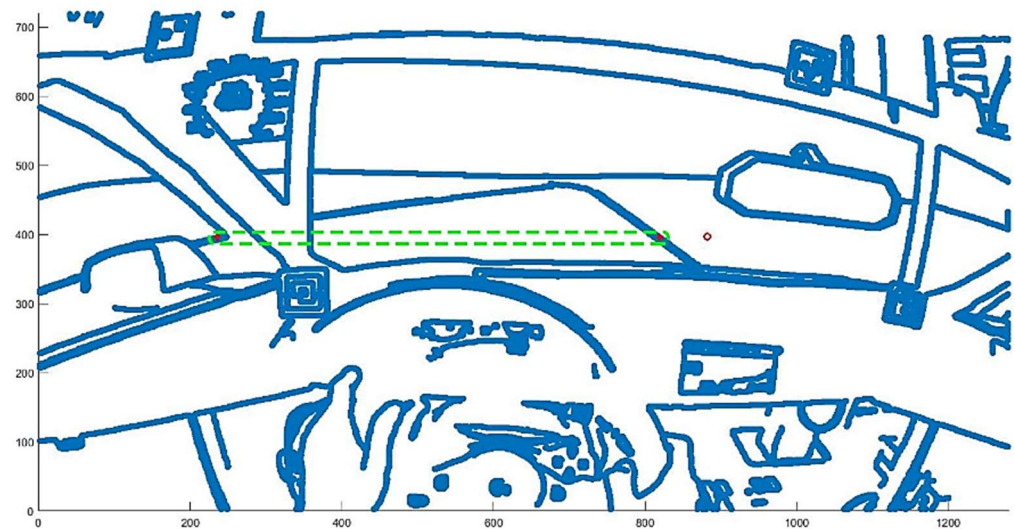


Figure 12. The dashed green line represents the selection window adjustment in critical cases. The filled red dots represent chosen road coordinates, while the red circle indicates the driver's gaze position.

Another guideline that was attempted to be implemented was locating the selection window as close as possible to the gaze position to appropriately understand the gaze's situation, whether inside or outside. This means all outcomes are correct and do not need a comparison test.

4. Results

The following investigations demonstrate how the results obtained using the previously mentioned method can be utilized to analyze driver visual behavior.

4.1. Analysis by Ratio and b per Driver

Figures 13 and 14 show each a multiple plot (2×2 subplots) by drivers of gazes for a rectilinear and a curvilinear segment, respectively. The two black stripes on the ratio- b plane identify the two roadsides.

On the X axis, there is ratio [%] (see Equation (1)); on the Y axis, absolute b [pixels]; and on the Z axis, the frequency. It is worth noting that (when the road section is constant, like in our case), due to perspective, when b is high, the gaze points close to the vehicle, and vice versa. When b is small, it means the gaze point is far from the vehicle. Hence, in those figures, the data closest to the X-axis are related to the farthest gazes. The two black stripes on the X-Y plane for $X = 0$ and $X = -1$ (100%) delimit the road, and the data between them are inside the road.

The dispersion of data is almost similar per driver. The frequency peaks are always inside the road, but some data are outside, mainly for the rectilinear segment. For the curvilinear segment, data outside are very scarce (see also Tables 3 and 4) and not very far from the roadsides (no more than 16 m against the 32 m in the rectilinear segment). Data are tendentially farther in the rectilinear segment. A clear example of this is in the subplot of Figure 14 for driver #4.

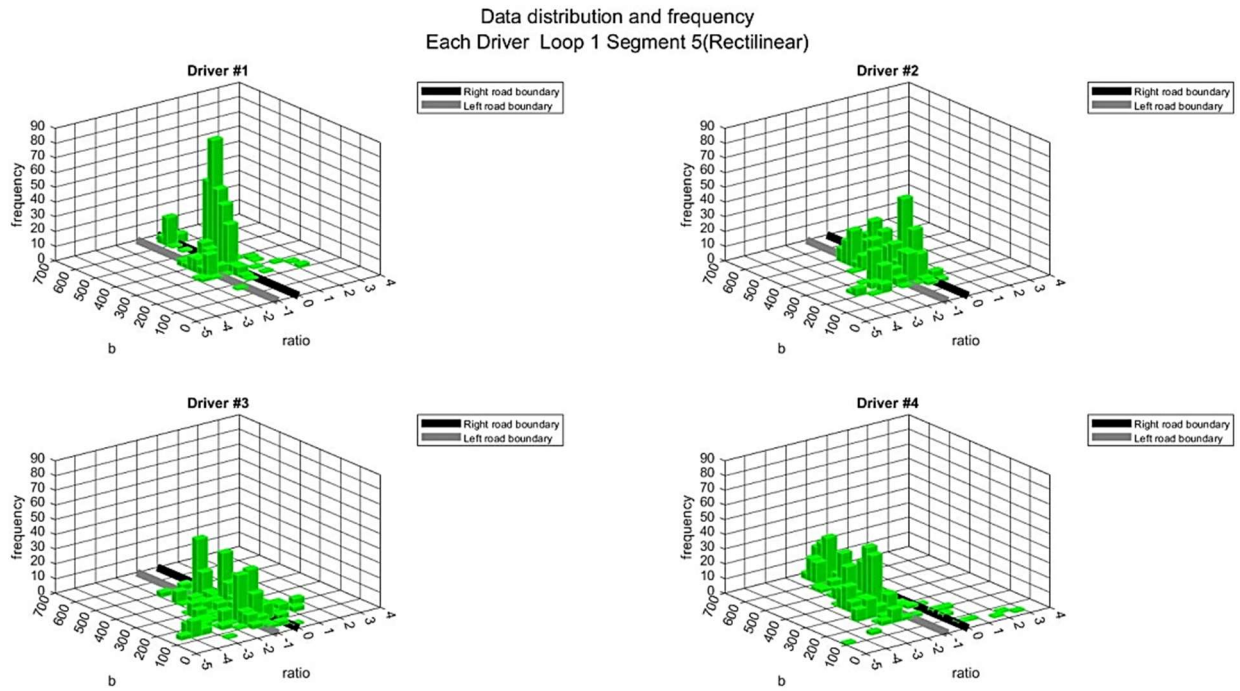


Figure 13. Gaze distribution by driver in the 3D space of ratio, b, and frequency for the rectilinear segment 5.

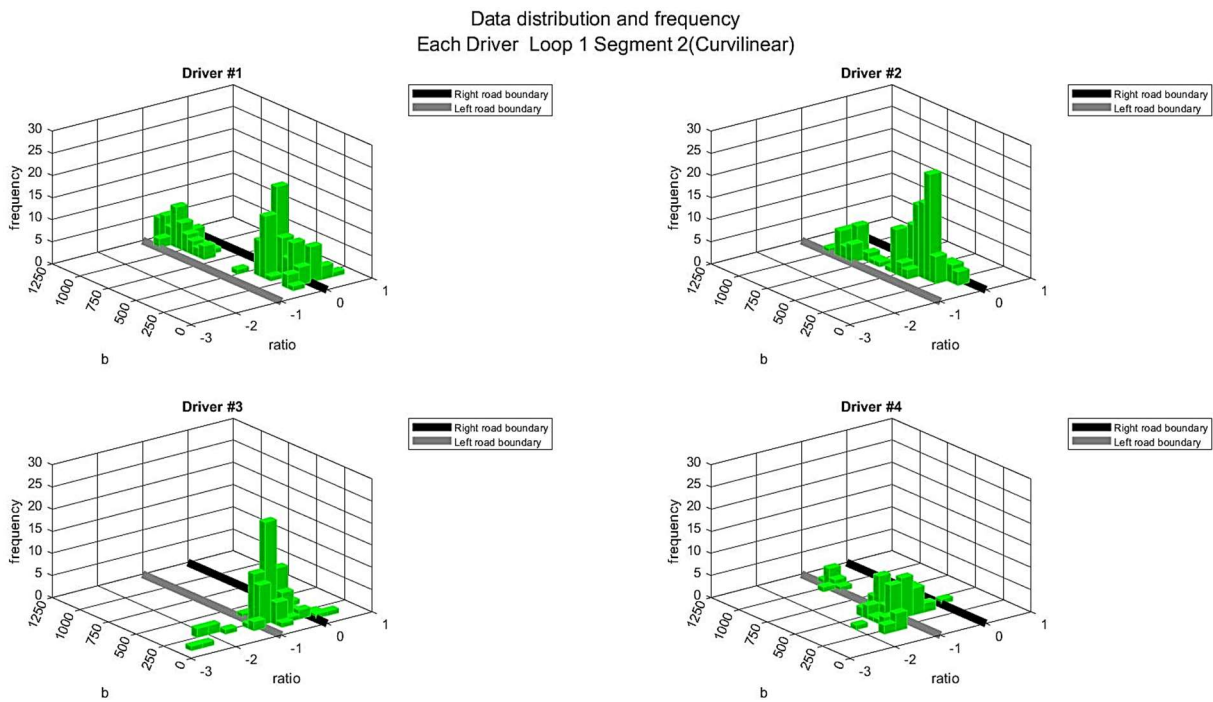


Figure 14. Gaze distribution by driver in the 3D space of ratio, b, and frequency for the curvilinear segment 2.

Table 3. Statistics of gaze distribution by driver in the 2D space of a' [m] for the rectilinear segment 5 and the curvilinear segment 2.

Segments	Driver #1			Driver #2			Driver #3			Driver #4		
	Mean	Median	Mode	Mean	Median	Mode	Mean	Median	Mode	Mean	Median	Mode
Segment 5, Rectilinear	-2.89	-2.25	-1.83	-6.02	-4.37	-2.91	-8.25	-6.93	-6.62	-10.0	-9.28	-6.62
Segment 2, Curvilinear	-2.37	-2.18	-1.44	-3.67	-3.25	-2.75	-2.96	-4.35	-4.20	-7.79	-7.82	-10.06

Table 4. Statistics of gazes within the road in the rectilinear segment 5 and the curvilinear segment 2.

Segments	Driver #1		Driver #2		Driver #3		Driver #4	
	% Inside	# of Frames	% Inside	# of Frames	% Inside	# of Frames	% Inside	# of Frames
Segment 5, Rectilinear	84.5%	434	68.5%	532	57.5%	540	34.0%	520
Segment 2, Curvilinear	88.0%	151	100.0%	151	84.5%	107	53.0%	90

4.2. Analysis by Section per Driver

This analysis focuses on the distribution of gazes along the road section. The data are the same as those from previous analyses plotted in a 3D graphic but projected and summed along the ratio plane. A detailed study of gaze distribution inside vs. outside the road, closer to the right or left roadside, is easier to carry out from these graphics.

Figures 15 and 16 show the distribution of gaze data for the rectilinear and curvilinear segments, respectively. Besides the different scale of frequency (due to the different number of available frames) and the differences by drivers, the two sets of distributions have a different structure: in the rectilinear segment, the shape of the distributions is mainly unimodal, though with a different mean by driver, whereas it tends to be bimodal in the curvilinear segment for some drivers.

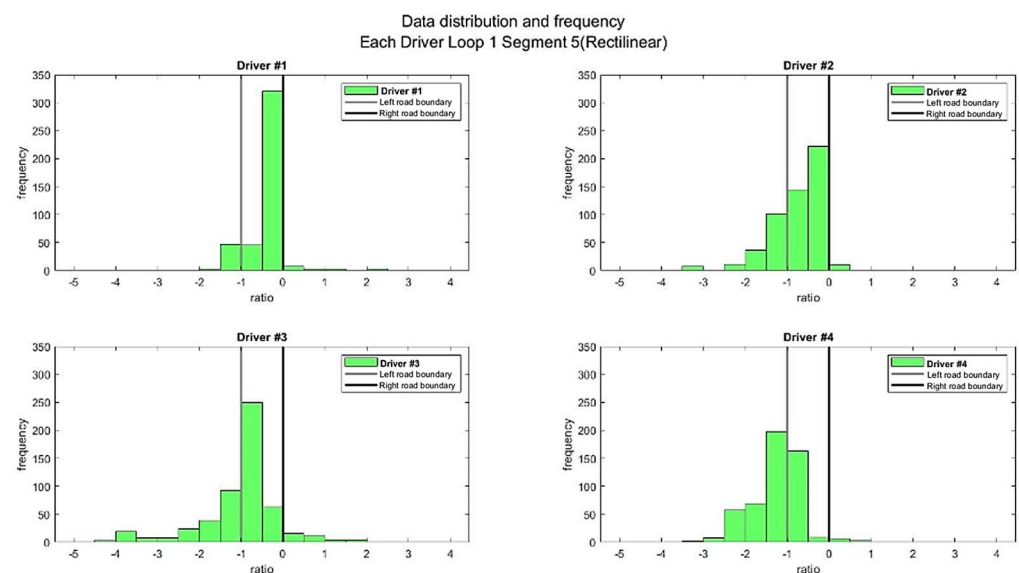


Figure 15. Gaze distribution by driver in the 2D space of ratio and frequency for the rectilinear segment 5.

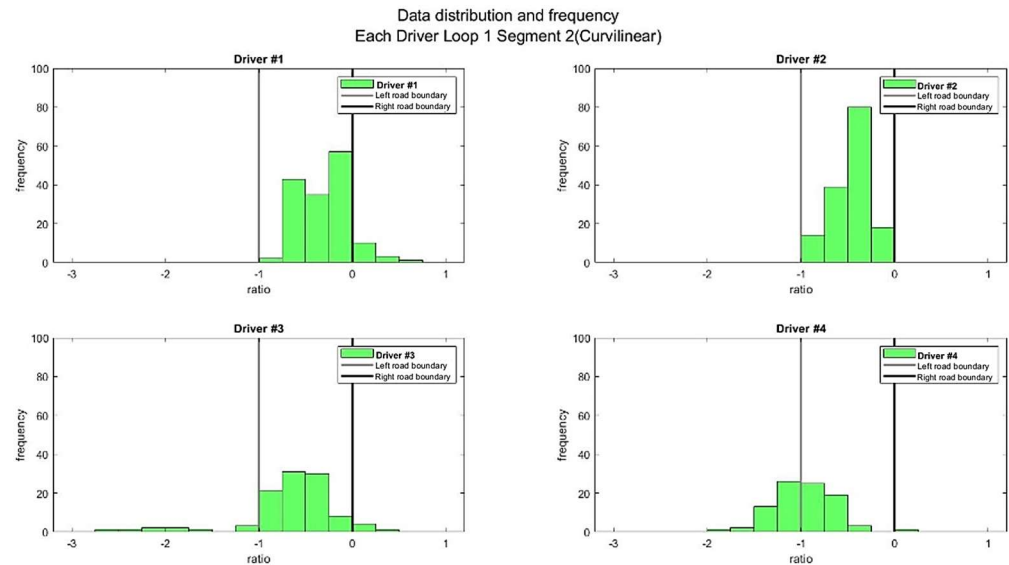


Figure 16. Gaze distribution by driver in the 2D space of ratio and frequency for the curvilinear segment 2.

Table 2 reports some statistics of a' (mean, median, and mode, calculated using b_{real} , the actual value of b , that is, the road section width). The differences between drivers are evident for all three quantities. The only feature common to all drivers is that the absolute values for the curvilinear segment are always less than those for the rectilinear one, and the mean is greater than the median, which in turn is greater than the mode (the only exception is the mode of driver #4). This confirms that the gaze distribution of data is not symmetric, has a peak closer to the roadside on the right than the mean and the median, and has a longer queue toward the environment on the left side of the road than that on the right. Except for driver #4, these statistical values are all inside the road section.

Notably, the mean, median, and mode values for the curvilinear segment are consistently lower in absolute value than those for the rectilinear segment (except for driver #4's mode value). This suggests that drivers tend to look more towards the center of the road during curvilinear sections, possibly due to the increased attentional demands of navigating curves and bends.

Table 4 reports the total number of frames used and their percentages with the gaze inside the road for a rectilinear and a curvilinear segment. In the rectilinear segment, the percentage of looking within the road is almost always lower than that in the curvilinear segment, though it varies much from driver to driver.

Looking at the histograms drawn for each driver (Figures 15 and 16), it is evident that some drivers glance more at the right road borderline, whereas others look more at the left road borderline. However, the gaze distribution is more concentrated near the roadsides, inside or outside the road, for the curved portion.

Figures 17 and 18 show the gaze sequence of driver #1 for the rectilinear and curvilinear segments, respectively. These data allow a dynamic analysis of gaze, which is not the aim of this paper, but it is reported to show the method's potential. Knowing how far or frequently a point on the scene is looked at can add further insight into driver behavior.

The chosen points on the left and right borderlines change as the driver's gaze shifts during the driving session. The road border coordinates were changed because of the selection window's placement and size adjustments. These adjustments were needed due to changes in the driver's view of the simulation path and variations in the road's geometry along the track, with more substantial variations occurring in curvilinear sections and milder ones in rectilinear sections.

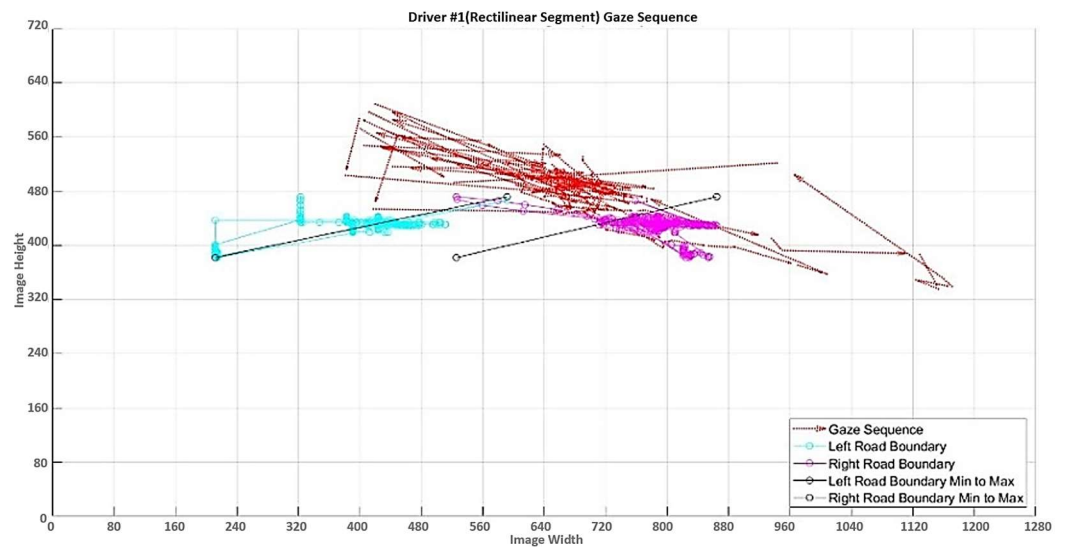


Figure 17. The gaze sequence of driver #1 for the rectilinear segment.

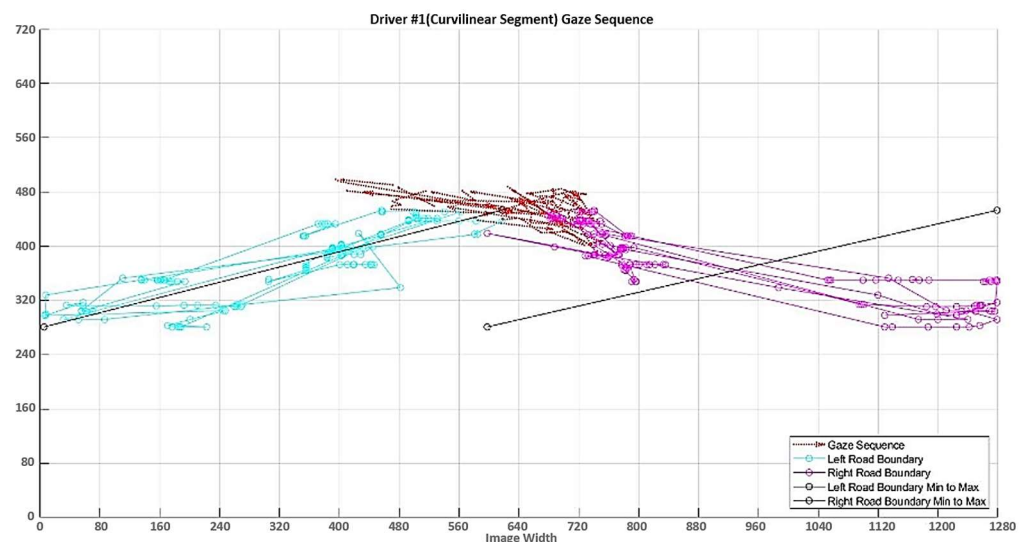


Figure 18. The gaze sequence of driver #1 for the curvilinear segment.

5. Discussion

The method proposed to analyze the eye-tracker data on gaze locations requires a series of data processing steps to overcome the lack of 3D information in the collected data.

As already argued, the lack of 3D vision means a lack of information about where the gaze position and road borders are in 3D space and the distance between them. Consequently, for all the reasons stated above, it is vital to set specific guidelines to overcome this significant limitation as much as possible. Of course, the link between the 2D images and the 3D model of the circuit can overcome this limitation, but it must be carefully planned before the simulations are integrated with them.

Accurately analyzing gaze position according to road borders requires consideration of the effect of perspective. Placing the road boundary coordinates in the same y-coordinate as the gaze or the projection of the gaze on the base of the building (when the gaze is on a building facade) is ideal. Please see Figure 7 for the cases mentioned above. However, this kind of placement can be time-consuming and sometimes not even possible in situations where the gaze or the projection of the gaze is not parallel to the road borders, such as when the driver is looking straight ahead to the horizon. To address this limitation, a “ratio” variable approach has been proposed, where the gaze is considered inside the road boundary if the ratio is between 0 and -1 , eliminating the need for parallel alignment.

Nevertheless, to ensure precise results in scenarios where the gaze or the projection of the gaze is not parallel to the road, it is essential to account for perspective by positioning the road boundary coordinates lower in the y -axis than the gaze coordinates to avoid misinterpretations of the gaze as being outside the road borders when it is inside. This proper adjustment is achieved by narrowing the selection window size in the y -axis for the road coordinates to ensure that the chosen road border coordinates are lower in the y -axis than the driver's gaze position.

Another critical aspect that should be considered when analyzing gaze position at road borders is appropriately adjusting the selection window in critical situations. For instance, when the driver's gaze is near the right borderline of the road, it is imperative to adjust the selection window to an appropriate size. This is particularly important when the driver is driving counterclockwise (in right-hand drive), as the perspective can lead to an erroneous interpretation of the gaze direction. Therefore, adjusting the selection window to an optimal size under such critical circumstances is essential to ensuring an accurate interpretation of the driver's gaze. Refer to Figure 13 to better understand the selection window adjustment in critical scenarios.

The difference between a counterclockwise and a clockwise circuit depends on the direction of circulation. In a right-hand circulation and a counterclockwise circuit, the driver must drive close to the roadside on the right, whereas in a left-hand circulation, he must drive close to the left roadside. The vehicle's trajectory and speed profile may be affected if the road section is wide enough (more than one lane).

Curvilinear segments are generally short, and fewer frames are available for analysis. Besides this, some of them could be unusable because the road line border is not visible due to either the perspective of a curvilinear stretch or the obstruction of the door pillar (for left curves) or the windscreen pillar (for right curves).

Outcomes show where the driver looks, outside or inside the road, depending on the driver's style. We can know where he is looking with a resolution limited only by perspective distortion, which cannot be controlled by our method. This effect is much less intense for the portions of images in the center of the scene than when the driver is looking inside the road section. The higher the distance from the roadside, the higher the distortion. The procedure has a further step in the presence of buildings or objects. It must identify where the gaze points; then, the vertical plane (the facade in the case of a building) on which the gaze is located must be identified, and along this plane, its projection on the ground determines the location of the gaze. This procedure is cumbersome, and besides the error introduced by perspective distortion, it can be affected by the difficulty of identifying the ground border. In any case, there is no alternative to this set of data. We decided to use only the projection of the gaze on the ground because the point on the facade is affected by a higher distortion than the corresponding projected point on the ground. It is worth noting that the method can also be applied to images collected by the same devices while driving in real life.

Anh Son et al. (2019) [52] quantified driver mental workload using a combined vestibular–ocular reflex (VOR) and optokinetic reflex (OKR) model, which is essential for maintaining stable vision while driving. However, their method's reliance on head movements presents a significant limitation, particularly as modern vehicle suspensions and improved road conditions reduce the necessary vibrations for accurate modeling. Their approach assumes that discrepancies between predicted and observed eye movements indicate cognitive distraction.

Our proposed method addresses this limitation by eliminating the need for head movements. We use an image-processing algorithm to link eye-tracker data with the simulation. While our research focus differs slightly, our method can assess drivers' attention allocation to road geometry, helping to detect distraction and analyze the impact of different road types. Despite differing specific aims, both studies aim to improve understanding of driver distraction and attention.

While we acknowledge the benefits of the Canny approach in our study, particularly its robustness in detecting weak edges amidst noise, the novelty of our method lies in its integration and adaptation of various components to analyze gaze positions concerning road borders. Our approach specifically addresses the challenge of analyzing gaze data without 3D information, a prevalent constraint in eye-tracker studies of this nature. We overcame this challenge by carefully considering perspective and introducing innovative adjustments such as the “ratio” variable approach and selection window adjustment. Additionally, our method seamlessly connects eye-tracker data with virtual reality simulation, tackling a significant challenge in such simulator environments.

While we drew from both older and recent literature, finding recent studies yielding robust results on road geometry analysis via gaze data was challenging. A gap persists between older studies and current driving conditions, despite newer research. Integrating vehicle technology and road infrastructure advancements could enhance driver behavior analysis, but few recent studies have explored this. However, filling this gap remained challenging, as did finding methods for accurately pinpointing driver focus in virtual environments lacking 3D information. To overcome this, we established a novel connection between gaze data and simulation, enabling a more precise examination of driver behavior concerning road geometry. Its versatility allows for application across diverse scenarios, such as assessing advertisement effectiveness along roadways and comparing distraction levels pre- and post-implementation of proposed urban layout changes.

Although our method has certain limitations, it addresses many challenges associated with 2D data collection. In the absence of 3D data, this represents the best achievable outcome. While acknowledging these limitations is essential to scientific research, refining the method for future applications is equally crucial. Although the process may be labor-intensive and not always yield consistent results, it represents a significant step forward in addressing a complex problem. We anticipate further advancements and iterations to enhance its efficiency and accuracy. Integrating AI, as demonstrated by Zemblys et al. (2017) [53], can potentially automate and improve our method, reducing labor intensity and increasing consistency by leveraging machine learning techniques for more robust and efficient analysis.

6. Conclusions

The proposed method hinges on image processing techniques to overcome most limitations due to the 2D images collected by the eye-tracker video camera. This holds with high accuracy for what concerns gazes inside the road, where distortion due to perspective is limited. For gazes outside the road, accuracy can be affected by perspective and the presence of buildings. The farther the facades of the buildings are from the road, the more uncertain the assessment of the coordinates of the gaze looking at them. This uncertainty can be solved only by using the 3D model of the scenery.

After the gazes are collected, their distribution over the road section and their temporal sequence are analyzed straightforwardly. This allows for an in-depth analysis of the driver’s behavior. This will be a future step of the research, which implies a different setup of the simulation experiments from that used in the presented work.

The current study quantitatively explores how drivers allocate their gaze positions relative to road curvature, significantly influencing safety behavior. While it may seem intuitive that drivers focus more on curves, quantifying this behavior provides valuable insights into attention distribution and informs strategies for designing safer road environments. It was realized by establishing a connection between eye-tracker data and virtual reality simulation, addressing a challenge in such simulator environments.

It is worth mentioning that the proposed method can also be applied to images collected in a naturalistic survey. However, future research will also consider a larger sample to improve the significance of the findings by considering different classes of drivers by age and different driving scenarios.

Author Contributions: Conceptualization, G.C. and L.M.; methodology, G.C. and L.M.; validation, L.M.; investigation, F.A.; writing—original draft, F.A.; writing—review and editing, G.C. and L.M.; supervision, G.C. and L.M. All authors have read and agreed to the published version of the manuscript.

Funding: This research received no external funding.

Institutional Review Board Statement: All subjects gave informed consent for inclusion before participating in the study. This study followed the Declaration of Helsinki, and the protocol was approved by the Ethics Committee of Politecnico di Milano (protocol code 35/2020, 2 December 2020).

Informed Consent Statement: Informed consent was obtained from all subjects involved in the study.

Data Availability Statement: The data presented in this study are available on request from the corresponding author.

Acknowledgments: This research was supported by the i.Drive Lab (<http://www.idrive.polimi.it/>), accessed on 20 April 2024). The authors thank all the survey participants for investing their time in this study.

Conflicts of Interest: The authors declare no conflicts of interest.

References

1. Magaña, V.C.; Scherz, W.D.; Seepold, R.; Madrid, N.M.; Pañeda, X.G.; Garcia, R. The Effects of the Driver's Mental State and Passenger Compartment Conditions on Driving Performance and Driving Stress. *Sensors* **2020**, *20*, 5274. [[CrossRef](#)] [[PubMed](#)]
2. World Health Organization. Global Status Report on Road Safety. 2018. Available online: <https://www.who.int/publications/item/9789241565684> (accessed on 1 April 2024).
3. European Commission. Best Practices in Road Safety, Publications Office. 2010. Available online: <https://data.europa.eu/doi/10.2832/16225> (accessed on 1 April 2024).
4. Longo, L. Designing Medical Interactive Systems Via Assessment of Human Mental Workload. In Proceedings of the 2015 IEEE 28th International Symposium on Computer-Based Medical Systems, Sao Carlos, Brazil, 22–25 June 2015; pp. 364–365.
5. Matton, N.; Paubel, P.-V.; Puma, S. Toward the Use of Pupillary Responses for Pilot Selection. *Hum. Factors* **2020**, *64*, 555–567. [[CrossRef](#)] [[PubMed](#)]
6. Benedetto, S.; Pedrotti, M.; Minin, L.; Baccino, T.; Re, A.; Montanari, R. Driver workload and eye blink duration. *Transp. Res. Part F Traffic Psychol. Behav.* **2011**, *14*, 199–208. [[CrossRef](#)]
7. Wang, Z.; Zheng, R.; Kaizuka, T.; Nakano, K. Relationship Between Gaze Behavior and Steering Performance for Driver–Automation Shared Control: A Driving Simulator Study. *IEEE Trans. Intell. Veh.* **2019**, *4*, 154–166. [[CrossRef](#)]
8. Chihara, T.; Kobayashi, F.; Sakamoto, J. Estimation of mental workload during automobile driving based on eye-movement measurement with a visible light camera. *Trans. JSME* **2020**, *86*, 19–326. [[CrossRef](#)]
9. Huang, L.; Liang, Z.; Suarez, D.L.; Wang, Z.; Wang, M. Effects of continuous nitrogen application on seed yield, yield components and nitrogen-use efficiency of *Leymus chinensis* in two different saline-sodic soils of Northeast China. *Crop Pasture Sci.* **2019**, *70*, 373–383. [[CrossRef](#)]
10. Kosch, T.; Hassib, M.; Woźniak, P.W.; Buschek, D.; Alt, F. Your Eyes Tell: Leveraging Smooth Pursuit for Assessing Cognitive Workload. In Proceedings of the 2018 CHI Conference on Human Factors in Computing Systems, Montreal, QC, Canada, 21–26 April 2018.
11. Young, K.; Salmon, P.; Cornelissen, M. Missing links? The effects of distraction on driver situation awareness. *Saf. Sci.* **2013**, *56*, 36–43. [[CrossRef](#)]
12. McEvoy, S.P.; Stevenson, M.R.; McCartt, A.T.; Woodward, M.; Haworth, C.; Palamara, P.; Cercarelli, R. Role of mobile phones in motor vehicle crashes resulting in hospital attendance: A case-crossover study. *BMJ* **2005**, *331*, 428. [[CrossRef](#)]
13. Neyens, D.; Boyle, L. The effect of distractions on the crash types of teenage drivers. *Accid. Anal. Prev.* **2007**, *39*, 206–212. [[CrossRef](#)]
14. Redelmeier, D.A.; Tibshirani, R.J. Association between Cellular-Telephone Calls and Motor Vehicle Collisions. *N. Engl. J. Med.* **1997**, *336*, 453–458. [[CrossRef](#)]
15. Tao, S.; Wu, X.; Wan, Y.; Zhang, S.; Hao, J.; Tao, F. Interactions of problematic mobile phone use and psychopathological symptoms with unintentional injuries: A school-based sample of Chinese adolescents. *BMC Public Health* **2016**, *16*, 88. [[CrossRef](#)] [[PubMed](#)]
16. Stanton, N.A.; Young, M.S.; Walker, G.H. *Cognitive Work Analysis: Applications, Extensions and Future Directions*; CRC Press: Boca Raton, FL, USA, 2015.
17. Green, P.R.; McDonald, C.C.; Van Horn, R.L. *Driver Distraction: Theory, Effects, and Mitigation*; CRC Press: Boca Raton, FL, USA, 2013.
18. Neale, V.L.; Klauer, S.G.; Knipling, R.R.; Dingus, T.A.; Holbrook, G.T.; Petersen, A. *The 100-Car Naturalistic Driving Study, Phase I—Experimental Design*; U.S. Department of Transportation: Washington, DC, USA, 2002.

19. Simons-Morton, B.G.; Guo, F.; Klauer, S.G.; Ehsani, J.P.; Pradhan, A.K. Keep your eyes on the road: Young driver crash risk increases according to duration of distraction. *J. Adolesc. Health Off. Publ. Soc. Adolesc. Med.* **2014**, *54* (Suppl. S5), S61–S67. [[CrossRef](#)]
20. Ibrahim, J.K.; Anderson, E.D.; Burris, S.C.; Wagenaar, A.C. State Laws Restricting Driver Use of Mobile Communications Devices: Distracted-Driving Provisions, 1992–2010. *Am. J. Prev. Med.* **2011**, *40*, 659–665. [[CrossRef](#)]
21. Klauer, S.G.; Guo, F.; Simons-Morton, B.G.; Ouimet, M.C.; Lee, S.E.; Dingus, T.A. Distracted Driving and Risk of Road Crashes among Novice and Experienced Drivers. *N. Engl. J. Med.* **2014**, *370*, 54–59. [[CrossRef](#)]
22. Liu, Z.; Yuan, W.; Ma, Y. Drivers' attention strategies before eyes-off-road in different traffic scenarios: Adaptation and anticipation. *Int. J. Environ. Res. Public Health* **2021**, *18*, 3716. [[CrossRef](#)]
23. Green, P. Where do drivers look while driving (and for how long). In *Human Factors in Traffic Safety*; Dewar, R.E., Olson, P.L., Eds.; Lawyers & Judges: Tucson, AZ, USA, 2002; pp. 77–110.
24. Olson, P.L.; Battle, D.S.; Aoki, T. Driver Eye Fixations under Different Operating Conditions, University of Michigan, Ann Arbor, Transportation Research Institute. 1989. Available online: <https://hdl.handle.net/2027.42/62169> (accessed on 1 April 2024).
25. Blaauw, G.J.; Godthelp, J.; Moraal, J. Driver's Lateral Control Strategy as Affected by Task Demands and Driving Experience. *SAE Trans.* **1977**, *86*, 3009–3017.
26. Jurgensohn, T.; Neculau, M.; Willumeit, H.P. Visual Scanning Pattern in Curve Negotiation. In *Vision in Vehicles III*; Gale, A.G., Gale, I., Brown, I., Haslegrave, C.M., Moorhead, I., Taylor, S.P., Eds.; Elsevier Science: Amsterdam, The Netherlands, 1991; pp. 171–178.
27. Jeong, H.; Liu, Y. Effects of non-driving-related-task modality and road geometry on eye movements, lane-keeping performance, and workload while driving. *Transp. Res. Part F Traffic Psychol. Behav.* **2019**, *60*, 157–171. [[CrossRef](#)]
28. Lehtonen, E.; Lappi, O.; Summala, H. Anticipatory eye movements when approaching a curve on a rural road depend on working memory load. *Transp. Res. Part F Traffic Psychol. Behav.* **2012**, *15*, 369–377. [[CrossRef](#)]
29. Nilsson, E.J.; Victor, T.; Ljung Aust, M.; Svanberg, B.; Lindén, P.; Gustavsson, P. On-to-off-path gaze shift cancellations lead to gaze concentration in cognitively loaded car drivers: A simulator study exploring gaze patterns in relation to a cognitive task and the traffic environment. *Transp. Res. Part F Traffic Psychol. Behav.* **2020**, *75*, 1–15. [[CrossRef](#)]
30. Bengler, K.; Bernasch, J.H.; Lowenau, J.P. Comparison of Eye Movement Behavior during Negotiation of Curves on Test Track and in BMW Driving Simulator. In Proceedings of the Annual Meeting of the Europe Chapter of the Human Factors and Ergonomics Society, Groningen, The Netherlands, 7–8 November 1996.
31. Zwahlen, H.T. Evaluation of Pushbutton Arrangements in Automobiles. *Proc. Hum. Factors Ergon. Soc. Annu. Meet.* **1993**, *37*, 969–973. [[CrossRef](#)]
32. Shinar, D.; McDowell, E.D.; Rockwell, T.H. Eye Movements in Curve Negotiation. *Hum. Factors* **1977**, *19*, 63–71. [[CrossRef](#)]
33. Hristov, B. Influence of Road Geometry on Driver's Gaze Behavior on Motorways. *E3S Web Conf.* **2019**, *97*, 01001. [[CrossRef](#)]
34. Chung, J.; Lee, H.; Moon, H.; Lee, E. The Static and Dynamic Analyses of Drivers' Gaze Movement Using VR Driving Simulator. *Appl. Sci.* **2022**, *12*, 2362. [[CrossRef](#)]
35. Duncan, J.; Williams, P.; Brown, I. Components of driving skill: Experience does not mean expertise. *Ergonomics* **1991**, *34*, 919–937. [[CrossRef](#)]
36. Lee, J.D. Technology and teen drivers. *J. Saf. Res.* **2007**, *38*, 203–213. [[CrossRef](#)]
37. Mayhew, D.R.; Simpson, H.M.; Pak, A. Changes in collision rates among novice drivers during the first months of driving. *Accid. Anal. Prev.* **2003**, *35*, 683–691. [[CrossRef](#)]
38. McGwin, G., Jr.; Brown, D.B. Characteristics of traffic crashes among young, middle-aged, and older drivers. *Accid. Anal. Prev.* **1999**, *31*, 181–198. [[CrossRef](#)]
39. McKnight, A.J.; McKnight, A.S. Young novice drivers: Careless or clueless? *Accid. Anal. Prev.* **2003**, *35*, 921–925. [[CrossRef](#)]
40. Pradhan, A.K.; Hammel, K.R.; DeRamus, R.; Pollatsek, A.; Noyce, D.A.; Fisher, D.L. Using Eye Movements To Evaluate Effects of Driver Age on Risk Perception in a Driving Simulator. *Hum. Factors* **2005**, *47*, 840–852. [[CrossRef](#)]
41. Crundall, D.E.; Underwood, G. Effects of experience and processing demands on visual information acquisition in drivers. *Ergonomics* **1998**, *41*, 448–458. [[CrossRef](#)]
42. Mourant, R.R.; Rockwell, T.H. Strategies of Visual Search by Novice and Experienced Drivers. *Hum. Factors* **1972**, *14*, 325–335. [[CrossRef](#)]
43. Summala, H.; Nieminen, T.; Punto, M. Maintaining Lane Position with Peripheral Vision during In-Vehicle Tasks. *Hum. Factors* **1996**, *38*, 442–451. [[CrossRef](#)]
44. Underwood, G.; Chapman, P.; Brocklehurst, N.; Underwood, J.; Crundall, D. Visual attention while driving: Sequences of eye fixations made by experienced and novice drivers. *Ergonomics* **2003**, *46*, 629–646. [[CrossRef](#)]
45. van Leeuwen, P.M.; Happee, R.; de Winter, J.C.F. Changes of Driving Performance and Gaze Behavior of Novice drivers During a 30-min Simulator-based Training. *Procedia Manuf.* **2015**, *3*, 3325–3332. [[CrossRef](#)]
46. Horng, W.-B.; Chen, C.-Y.; Chang, Y.; Fan, C.-H. Driver fatigue detection based on eye-tracking and dynamic template matching. *IEEE Int. Conf. Netw. Sens. Control* **2004**, *1*, 7–12. [[CrossRef](#)]
47. Ohn-Bar, E.; Trivedi, M.M. Hand Gesture Recognition in Real Time for Automotive Interfaces: A Multimodal Vision-Based Approach and Evaluations. *IEEE Trans. Intell. Transp. Syst.* **2014**, *15*, 2368–2377. [[CrossRef](#)]

48. Zhang, F.; Su, J.; Geng, L.; Xiao, Z. Driver Fatigue Detection Based on Eye State Recognition. In Proceedings of the 2017 International Conference on Machine Vision and Information Technology (CMVIT), Singapore, 17–19 February 2017; pp. 105–110. [[CrossRef](#)]
49. Xi, H.; Zhang, Y. Detection of Safety Features of Drivers Based on Image Processing. In Proceedings of the 18th COTA International Conference of Transportation Professionals, Beijing, China, 5–8 July 2018.
50. CarMaker. Available online: <https://ipg-automotive.com/> (accessed on 1 April 2024).
51. Canny, J. A Computational Approach to Edge Detection. *IEEE Trans. Pattern Anal. Mach. Intell.* **1986**, *PAMI-8*, 679–698. [[CrossRef](#)]
52. Anh Son, L.; Suzuki, T.; Aoki, H. Evaluating driver cognitive distraction by eye tracking: From simulator to driving. *Transp. Res. Interdiscip. Perspect.* **2019**, *4*, 100087. [[CrossRef](#)]
53. Zemblys, R.; Niehorster, D.; Komogortsev, O.; Holmqvist, K. Using machine learning to detect events in eye-tracking data. *Behav. Res. Methods* **2017**, *50*, 160–181. [[CrossRef](#)]

Disclaimer/Publisher’s Note: The statements, opinions and data contained in all publications are solely those of the individual author(s) and contributor(s) and not of MDPI and/or the editor(s). MDPI and/or the editor(s) disclaim responsibility for any injury to people or property resulting from any ideas, methods, instructions or products referred to in the content.